Available online at www.sciencedirect.com
SCIENCE DIRECT
Journal of the European Ceramic Society 26 (2006) 1883–1887
www.elsevier.com/locate/jeurceramsoc

Effect of CeO_2 on the sintering behaviour, cation order and properties of $Ba_3Co_{0.7}Zn_{0.3}Nb_2O_9$ ceramics

F. Azough, C. Leach, R. Freer *

Manchester Materials Science Centre, School of Materials, University of Manchester, UMIST, Grosvenor Street, Manchester M1 7HS, UK

Available online 17 October 2005

Abstract

The effect of low-level CeO_2 addition and cooling rate on sintering, microstructures, phase formation, 1:2 ordering and microwave dielectric properties of $Ba_3Co_{0.7}Zn_{0.3}Nb_9$ (BCZN) was investigated. It was found that low levels doping of CeO_2 (up to 0.5 wt.%) could significantly improve densification of the specimens and their properties. Dielectric properties of CeO_2-doped samples were sensitive to 1:2 ordering in the B-site. Slow cooling after sintering improved the unloaded quality factor ($Q \times f$ values) significantly. The B-site ordering parameter (S) and lattice constant (c/a) values increased as the cooling rate decreased. $Ba_5Nb_4O_{15}$ (5/0/4) and $Ba_8(Co,Zn)_1Nb_6O_{24}$ (8/1/6) secondary phases were found on the surface of all the samples. At 0.4 wt.% CeO_2 the specimens showed maximum $Q \times f$ of 84,000 GHz attributed to high density and the degree of cation ordering.

Keyword: Microwave dielectrics

1. Introduction

Ceramic dielectrics are used extensively in microwave communication systems including cellular phone, direct broadcasting satellite and global positioning systems. The advantage of using microwave dielectric ceramics is the size reduction of microwave components. Requirements for these dielectric materials include a high relative permittivity ($\varepsilon_{r)}$, low dielectric loss (high $Q \times f$ value) and a near-zero temperature coefficient of resonant frequency (τ_f). These three parameters are related to the size, frequency selectivity and temperature stability of the system, respectively. To satisfy the demands of microwave circuit designs, each dielectric property should be precisely controlled. Several complex perovskites ceramics $A(B'_{1/3}B''_{2/3})O_3$ ($B' = Zn$, Co, Ni or Mg; $B'' = Ta$ or Nb) have attracted a great deal of attention due to their very low losses. Ta-based complex perovskite materials such as $Ba_3Zn_1Ta_2O_9$ and $Ba_3Mg_1Ta_2O_9$ have been used commercially[1,2] but Ta_2O_5 is more expensive than Nb_2O_5. A number of Nb-based complex perovskite materials have been reported in the scientific literature.[3–5] Amongst these materials, $Ba_3Co_{0.7}Zn_{0.3}Nb_2O_9$ (BCZN) possesses a high relative permittivity ($\varepsilon_r \sim 34.5$), a high quality factor ($Q \times f = 56{,}000$–$85{,}000$ GHz) and small temperature coefficient of resonant frequency ($\tau_f \sim 0$).[4,6,7] However, to obtain dense ceramics at temperatures below 1450 °C, a sintering aid is required.

Ceria has a relative permittivity, (ε_r), of 23, a high dielectric quality factor, $Q \times f$ up to 60,000 GHz with a large temperature coefficient of resonant frequency,[8] τ_f, of −53 ppm/°C. The effectiveness of the additions on sinterability and microwave dielectric properties of niobium based 1:1 type complex perovskites has been reported.[9] The niobium-based complex perovskites undergo an order–disorder transition below the sintering temperature. Therefore, the cooling rate after sintering may affect the quality factor by altering the degree of 1:2 order.

This investigation is concerned the effect of CeO_2 and cooling rate on the microwave dielectric properties, particularly the $Q \times f$ values, of $Ba_3Co_{0.7}Zn_{0.3}Nb_2O_9$ ceramics.

2. Experimental

Specimens were prepared by a conventional mixed oxide route. High-purity (>99.9%) $BaCO_3$, ZnO, Nb_2O_5 and CeO_2 were used as raw materials. The powders were weighed according to the composition $Ba_3Co_{0.7}Zn_{0.3}Nb_2O_9$. They were mixed in propan-2-ol with zirconia media for 18 h, calcined at 1100 °C for 4 h, then CeO_2 (up to 0.5 wt.%) was added and wet milled for

* Corresponding author. Tel.: +44 161 306 3564; fax: +44 161 200 8877.
E-mail address: Robert.Freer@manchester.ac.uk (R. Freer).

0955-2219/$ – see front matter © 2005 Elsevier Ltd. All rights reserved.
doi:10.1016/j.jeurceramsoc.2005.09.016

18 h and dried. Pellets were formed by pressing powders in steel dies (20 mm diameter) at a pressure of 100 MPa. These were sintered at 1450 °C for 4 h in air and cooled at 60 °C/h. Samples containing 0.35 wt.% CeO_2 were cooled at rates of 360, 90, 60, 30 and 5 °C/h after sintering at 1450 °C for 4 h in air. The final dimensions of these specimens were approximately 15.5 mm in diameter and 9 mm thick.

Microstructural observation of the sintered ceramics was performed by means of scanning electron microscopy (SEM) (Philips XL30). The sintered surfaces of ceramics were ground (to 1200 grade SiC) and polished (to 1 μm diamond paste). The samples were then coated with carbon prior to SEM analysis.

The crystal structures were examined by X-ray diffraction (Philips Analytical, X'pert-MPD) employing Cu $K\alpha_1$ radiation under the conditions 50 kV and 40 mA. The samples were scanned at 0.04° intervals of 2θ in the range 10–70°; the scan rate was 0.01° 2θ/s.

TEM specimens were prepared from the sintered ceramics, after lapping and polishing to form 3 mm diameter discs. The discs were dimpled to 30 μm thickness in the centre and then thinned to electron transparency with a Gatan Precision Ion Polishing System. The specimens were investigated using a Tecnai G2 TEM operating at 300 kV.

The dielectric properties (ε_r and $Q \times f$) were determined by the parallel plate method.[10] The τ_f values were determined using a silver-plated, aluminum cavity at temperatures between −10 and +60 °C.

3. Results and discussion

After sintering the BCZN ceramics it was noted that all the specimens contained secondary surface phases. We report first the characteristics of the matrix (i.e., BCZN) phase and then the surface phases.

3.1. The primary BCZN phase

The density of undoped BCZN ceramics after sintering at 1450 °C was only 70% theoretical. Addition of 0.2 wt.% CeO_2 increased the sintered density to 90% theoretical. At higher levels of CeO_2, densities over 95% of the theoretical were achieved (Fig. 1).

X-ray diffraction (XRD) examination of sintered products revealed a simple cubic structure for undoped BCZN. In contrast, for all samples prepared with additions of ceria, which achieved higher densities, a 1:2 ordered structure was observed. In order to assess the effect of ordering on dielectric properties, specimens prepared with additions of 0.35 wt.% CeO_2 were cooled at different rates after sintering. Fig. 2 shows XRD spectra of BCZN (+0.35 wt.% CeO_2) cooled at 360 and 30 °C/h. Both XRD spectra are characteristic of a 1:2 type, ordered hexagonal structure. The superlattice reflections, such as those at 17.6° and 25° 2θ, originate from 1:2 cation ordering, and were visible in all the high-density samples. However, the relative intensity of superlattice peaks increased as the cooling rate decreased to 30 °C/h. Further reduction of the cooling rate to 5 °C/h did not have any significant effect on the intensity of the superlattice reflections.

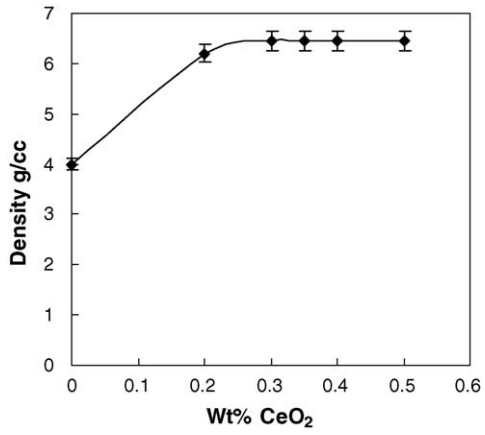

Fig. 1. Density of sintered BCZN ceramics as a function of wt.% CeO_2 in formulation.

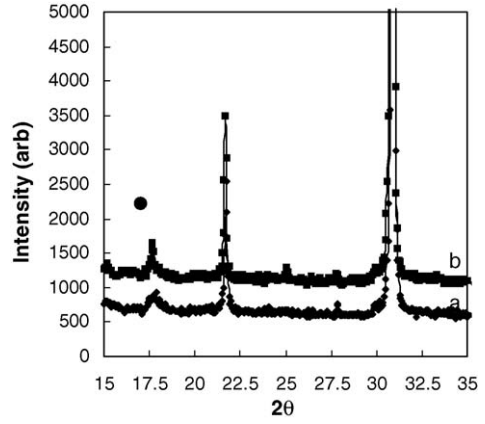

Fig. 2. X-ray diffraction spectra for BCZN ceramics prepared with addition of 0.35 wt.% CeO_2. Specimens were cooled at 360 and 30 °C/h after sintering. (●) Superlattice peak (a) cooled at 360 °C/h; (b) cooled at 30 °C/h.

The degree of ordering may conveniently be described in terms of the B-site ordering parameter (S). This was determined from the (1 0 0) superlattice reflection using Eq. (1)[11]:

$$S = \left\{ \frac{[I_{(100)}/I_{(110)} + I_{(102)} + I_{(012)}]\text{obs.}}{[I_{(100)}/I_{(110)} + I_{(102)} + I_{(012)}]\text{cal.}\}^{1/2}} \right\} \quad (1)$$

where $[I_{(100)}/I_{(110)} + I_{(102)} + I_{(012)}]_{\text{obs.}}$ is the ratio of the observed intensity of the (1 0 0) superlattice peaks (originating from ordering) in comparison to that of (1 1 0), (1 0 2) and (0 2 1) reflections from the subcell; $[I_{(100)}/I_{(110)} + I_{(102)} + I_{(012)}]_{\text{cal.}}$ is the corresponding ratio calculated from the from the fully ordered structure.

Fig. 3 shows the ordering parameter (S) and c/a values (ratio of lattice parameters c and a) as a function of cooling rate. Both S and c/a increased as the cooling rate decreased to 30 °C/h. The maximum value of the ordering parameter S was 0.9. Further reduction of the cooling rate did not significantly affect either parameter. The development of 1:2 ordering causes lattice distortion in the hexagonal unit cell. The distortion was evaluated in terms of the changes in the (4 2 2) and (2 2 6) reflections. Fig. 4 shows a magnified section of XRD spectra for samples cooled at 360, 90, 60 and 30 °C/h after sintering, revealing changes in the

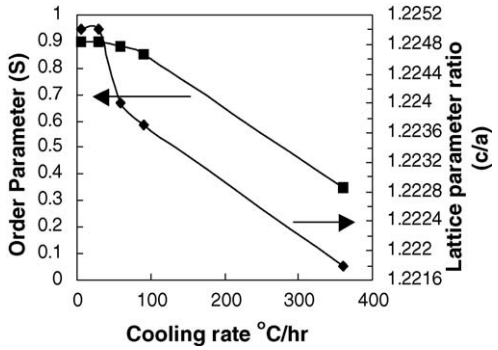

Fig. 3. Ordering parameter and *c*/*a* ratio for BCZN ceramic (prepared with addition of 0.35 wt.% CeO_2) as a function of cooling rate after sintering.

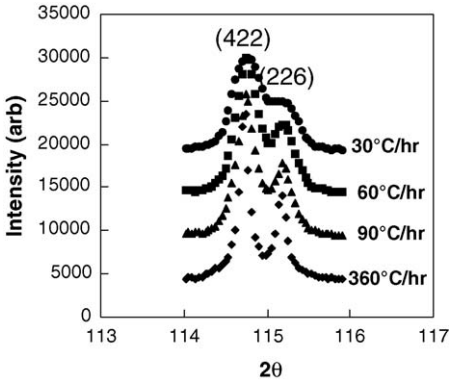

Fig. 4. Detail of X-ray diffraction spectra for BCZN ceramics (prepared with addition of 0.35 wt.% CeO_2) showing change in (4 2 2) and (2 2 6) diffraction peaks as a function of cooling rate (360, 90, 60, and 30 °C/h).

(4 2 2) and (2 2 6) diffraction peaks. The broadening of the (4 2 2) and (2 2 6) peaks start as the cooling rate decreases to 60 °C/h and is more evident as the cooling rate reduces to 30 °C/h. The XRD spectra for samples cooled at 5 °C/h are very similar to that for sample cooled at 30 °C/h.

Further information about the nature of the ordering in BCZN ceramics was gained by high-resolution TEM. Fig. 5 shows a HRTEM image of BCZN + 0.35 wt.% CeO_2 ceramic cooled at 60 °C/h. The grain is viewed along the $<1\,1\,0>_{cubic}$ zone axis. Ordered domains can be seen in the image; the domain

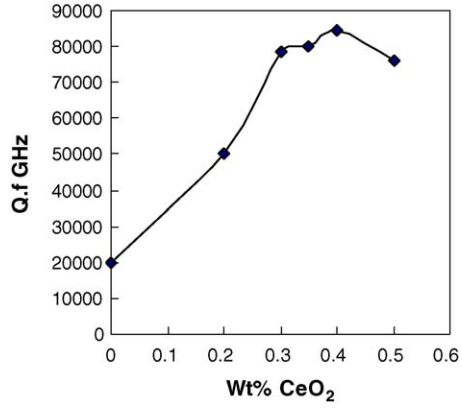

Fig. 5. HRTEM image of BCZN +0.35 wt.% CeO_2 ceramic cooled at 60 °C/h after sintering. Domains A and B are identified in the figure.

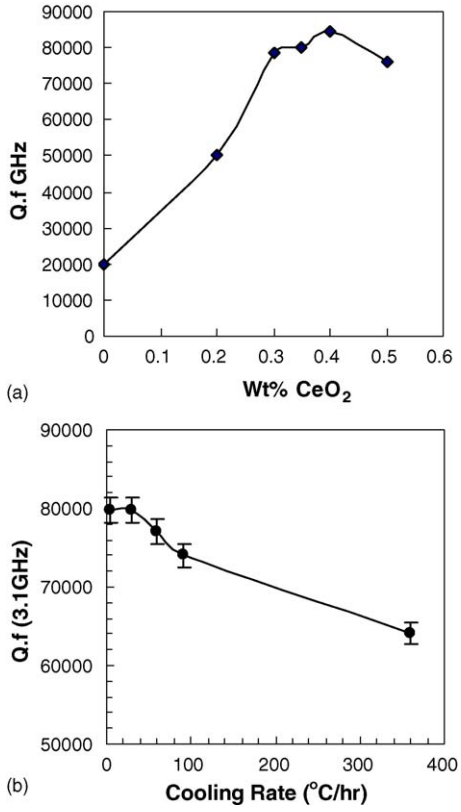

Fig. 6. $Q \times f$ values of BCZN ceramics (a) as a function of CeO_2 in starting formulation and (b) as a function of cooling rate after sintering (samples prepared with 0.35 wt.% CeO_2).

sizes are between 60 and 100 Å. Three types of domain boundaries are observed: type I between domains A and B with a displacement vector of $v = 1/2d_{(1\,0\,0)\,cubic}$; type II between A and C with a displacement vector of $1/2d_{(1\,1\,0)\,cubic}$; type III is a twin-type boundary with a twin angle of approximately 108°, which corresponds to the angle between {1 1 1} planes.

Fig. 6a shows $Q \times f$ values of BCZN ceramics as a function of ceria content. In the low-density, undoped BCZN ceramics the $Q \times f$ value is exceptionally low (~20,000). With increasing CeO_2 in the starting formulation there is a rapid increase of $Q \times f$ to 50,000 and then stabilizes at ~80,000. This increase in part reflects the increase in density (Fig. 1), but also the transition from a disordered cubic structure to 1:2 ordering of cations in a hexagonal structure. The XRD data showed that ordering, described in terms of the parameter *S*, increased to a maximum value of 0.9 as the cooling rate after sintering was reduced to 30 °C/h (Fig. 3). As anticipated, the dielectric $Q \times f$ values also changed with cooling rate after sintering (Fig. 6b). Rapidly cooled samples (i.e., 360 °C/h) with a low degree of 1:2 order had moderately high $Q \times f$ values of 62,000 (Fig. 6b). Reducing the cooling rate to 30 °C/h increased the $Q \times f$ values to the maximum value of 80,000. Further reduction of the cooling rate did not increase the $Q \times f$ values; this is consistent with the variation in the degree of ordering with cooling rate (Fig. 3). The relative permittivity (ε_r) and τ_f values of the dense samples were comparatively insensitive to processing

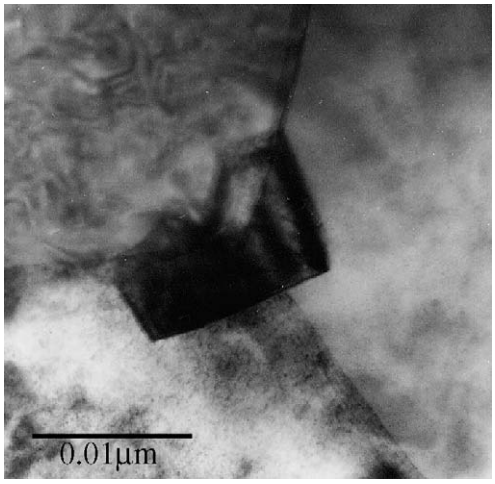

Fig. 7. TEM image of triple-point region in BCZN +0.35 wt.% CeO_2 ceramic cooled at 30 °C/h.

conditions (cooling rate and CeO_2 additions) and were ~34.5 and <1 ppm/°C, respectively.

Thus, it is clear that the improvements in the $Q \times f$ values of ceramics prepared with additions of CeO_2 are in response to increases in both densification and cation ordering. In order to clarify the role of ceria and the possibility of a Ce-rich component acting as liquid-phase sintering aid, TEM analysis was conducted on a slowly cooled BCZN + 0.35 wt.% CeO_2 sample. Fig. 7 shows a TEM image in the region of a triple point, where the additional phase is approximately 0.01 μm in size. EDS analysis suggests that the main component of the triple phase is ceria. Due to the small size of this phase and the contribution to EDS from the adjacent BCZN grains, unambiguous quantitative analysis is difficult. However, the Ba/Nb ratio in the triple-point phase is greater than the Ba/Nb ratio of the BCZN grains suggesting this additional phase is rich in CeO_2–BaO. Guha and Kolar[12] investigating the BaO–CeO_2 phase diagram noted a eutectic at 1440 °C for BaO-rich compositions and one at 1480 °C for CeO_2-rich compositions. The present findings, indicating liquid-phase formation during sintering BCZN–CeO_2 compositions at 1450 °C, are consistent with the data of Guha and Kolar. It is possible that the presence of ZnO plus Nb_2O_5 would further depress the melting temperature of the system below 1440 °C.

3.2. Secondary phases in BCZN ceramics

Fig. 8 shows an XRD spectrum of the as-fired surface of a BCZN ceramic prepared with 0.35 wt.% CeO_2. The spectrum can be indexed as mixture of two phases; $Ba_8(Co,Zn)_1Nb_6O_{24}$ and $Ba_5Nb_4O_{15}$. The formation of these two phases is due to the loss of zinc and cobalt during the sintering process. $Ba_8(Co,Zn)_1Nb_6O_{24}$ is a new type of complex perovskite and is isostructural with $Ba_8Ni_1Nb_6O_{24}$[13] and $Ba_8Zn_1Nb_6O_{24}$.[14] $Ba_5Nb_4O_{15}$ is a cation-deficient perovskite related to $A_nB_{n-1}O_{3n}$-type compounds[15] and has good microwave dielectric properties: $\varepsilon_r = 41$, $Q \times f$ value = 57,000 GHz and τ_f of +78 ppm/°C.[16]

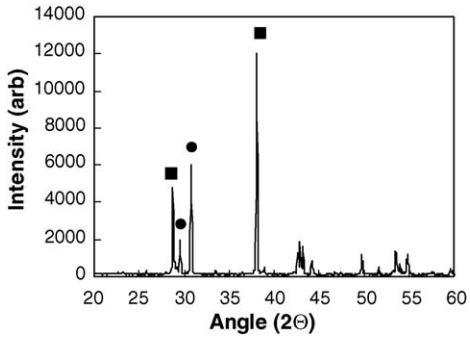

Fig. 8. X-ray diffraction spectrum of as-fired surface of BCZN +0.35 wt.% CeO_2 ceramic. (●) $Ba_8(Co,Zn)_1Nb_6O_{24}$; (■) $Ba_5Nb_4O_{15}$.

Fig. 9. SEM micrograph of as-fired surface of BCZN +0.35 wt.% CeO_2 ceramic.

SEM imaging (Fig. 9) with EDS analysis confirmed that CeO_2-doped BCZN ceramics exhibited two distinct secondary phases on the surface of the ceramics; needle-shaped grains and plate-shaped, rounded grains. EDS analysis of a thin foil (TEM) sample prepared from the surface of a BCZN +0.35 wt.% CeO_2 sample indicated that the Ba/(Co,Zn)/Nb ratio in the needle shape grains (Fig. 9) is approximately 8/1/6 suggesting the formula of $Ba_8(Co, Zn)_1Nb_6O_{24}$. For the primary grains, the Ba/(Co,Zn)/Nb ratio is about 3/1/2 suggesting a formula of $Ba_3(Co,Zn)_1Nb_2O_9$. Finally, the Ba/(Co,Zn)/Nb ratio for the plate-shaped grains (Fig. 9) is approximately 5/0/4 suggesting the formula of $Ba_5Nb_4O_{15}$ for this phase. The EDS data corroborates the findings from XRD analysis. Whilst the aim in most ceramics is to remove secondary surface phases, these Zn-deficient phases appear to be beneficial to the dielectric properties of the BCZN ceramics.

4. Conclusions

High-density BCZN ceramics, with a high degree of 1:2 cation order, were prepared with the aid of additions of cerium oxide. BCZN ceramics prepared with 0.4 wt.% CeO_2, sintered at 1450 °C for 4 h and cooled at 60 °C/h, possess excellent microwave dielectric properties: ε_r ~34.5, $Q \times f$ ~84,000 at 4 GHz and τ_f was close to zero.

At triple points a (Ce–Ba)-rich phase was detected. This is believed to be the residue of a liquid phase that assisted densification.

Zinc-deficient secondary phases $Ba_5Nb_4O_{15}$ and $Ba_8(Co,Zn)_1Nb_6O_{24}$ were detected on the surfaces of all samples as a result of zinc volatilisation during sintering.

Acknowledgements

The financial support of EPSRC through GR/R72655/01 and the assistance of Filtronic Ltd. with microwave measurements are gratefully acknowledged.

References

1. Matsumoto, H., Tamura, H. and Wakino, K., $Ba(Mg,Ta)O_3$–$BaSnO_3$ high-Q dielectric resonator. *Jpn. J. Appl. Phys.*, 1991, **30**(9B), 2347–2349.
2. Reaney, I. M., Wise, P. L., Qazi, I., Miller, C. A., Price, T. J., Cannell, D. S. *et al.*, Ordering and quality factor in $0.95BaZn_{1/3}Ta_{2/3}O_3$-$0.05SrGa_{1/2}Ta_{1/2}O_3$ production resonators. *J. Eur. Ceram. Soc.*, 2003, **23**, 3021–3034.
3. Azough, F., Leach, C. and Freer, R., Effect of cation order microwave dielectric properties of $Ba(Zn_{1/3}Nb_{2/3})O_3$ ceramics. *Key Eng. Mater.*, 2002, **264–268**, 1153–1156.
4. Azough, F., Leach, C. and Freer, R., The effect of additives and processing parameters on the microstructure and microwave dielectric properties of Ba(Me1/3Nb2/3)O3 complex perovskites (Me = Zn, Co, Ni and Mg). Presented at *Microwave Materials and their Applications (MMA20002)*, 1–3 September, York, UK, 2002 (poster 23).
5. Fukui, T., Sakurai, C. and Okuyama, M., Preparation of $Ba(Mg_{1/3}Nb_{2/3})O_3$ ceramics as microwave dielectrics through alkoxide–hydroxide route. *J. Mater. Res.*, 1992, **7**(7), 1883–1887.
6. Endo, K., Fujimoto, K. and Murakawa, K., Dielectric properties of ceramics in $Ba(Co_{1/3}Nb_{2/3})O_3$–$Ba(Zn_{1/3}Nb_{2/3})O_3$ solid solutions. *J. Am. Ceram. Soc.*, 1987, **70**(9), C-215–C-218.
7. Ahn, C.-W., Jang, H.-J., Nahm, S., Park, H.-M. and Lee, H.-J., Effect of microstructure on the microwave dielectric properties of $Ba(Co_{1/3}Nb_{2/3})O_3$ and $(1-x)Ba(Co_{1/3}Nb_{2/3})O_3$–$xBa(Zn_{1/3}Nb_{2/3})O_3$ solid solutions. *J. Eur. Ceram. Soc.*, 2003, **23**, 2473–2478.
8. Sebastian, M. T., Santha, N., Bijumon, P. V., Axelsson, A. K. and Alford, N. M., Microwave dielectric properties of $(1-x)CeO_2$–$xCaTiO_3$ and $(1-x)CeO_2$–xSm_2O_3 Ceramics. *J. Eur. Ceram. Soc.*, 2004, **24**, 2583–2589.
9. Khalam, L. A., Sreemoolanathan, H., Ratheesh, R., Mohanan, P. and Sebastian, M. T., Preparation, characterization and microwave dielectric properties of $Ba(B'_{1/2}Nb_{1/2})O_3$ B′ = La, Pr, Nd, Sm, Eu, Gd, Tb, Dy, Ho, Y, Yb and In ceramics. *Mater. Sci. Eng.*, 2004, **B107**, 264–270.
10. Hakki, B. W. and Coleman, P. D., A dielectric resonator method of measuring inductive capacitance in the millimetre range. *IEEE Trans. Mirowave Theory Tech.*, 1980, **MTT-18**, 402–410.
11. Davis, P. K., Tong, J. and Negas, T., Effect of ordering-induced domain boundaries on low-loss $Ba(Zn_{1/3}Nb_{2/3})O_3$–$BaZrO_3$ perovskite microwave dielectrics. *J. Am. Ceram. Soc.*, 1997, **80**(7), 1724–1740.
12. Guha, J. P. and Kolar, D., The system BaO–CeO_2. *J. Mater. Sci.*, 1971, **6**, 1174–1177.
13. Abakumov, A. M., Tendeloo, G. V., Scheglov, A. A., Shpanchenko, R. V. and Antipov, E. V., The crystal structure of $Ba_8Ni_1Nb_6O_{24}$: cation ordering in hexagonal perovskites. *J. Solid State Chem.*, 1966, **125**, 102–107.
14. Azough, F. and Freer, R., The crystal structure and dielectric properties of $Ba_8Zn_1Nb_6O_{24}$ ceramics, unpublished.
15. Vanderah, T. A., Collins, T. R., Wong-Ng, W., Roth, R. S. and Farber, I., Phase equilibria and crystal chemistry in the BaO–Al_2O_3–Nb_2O_5 and BaO–Nb_2O_5 systems. *J. Alloys Compd.*, 2003, **346**, 116–128.
16. Ratheesh, R., Sebastian, M. T., Mohanan, P., Tobar, M. E., Hartnett, J., Woode, R. *et al.*, Microwave characterisation of $BaCe_2Ti_5O_{15}$ and $Ba_5Nb_4O_{15}$ ceramic dielectric resonators using whispering gallery mode method. *Mater. Lett.*, 2000, **45**(5), 279–285.